BIT

CrossMark

Spectral properties of flipped Toeplitz matrices and related preconditioning

M. Mazza[1] · **J. Pestana**[2]

Abstract

In this work, we investigate the spectra of "flipped" Toeplitz sequences, i.e., the asymptotic spectral behaviour of $\{Y_n T_n(f)\}_n$, where $T_n(f) \in \mathbb{R}^{n \times n}$ is a real Toeplitz matrix generated by a function $f \in L^1([-\pi, \pi])$, and Y_n is the exchange matrix, with 1s on the main anti-diagonal. We show that the eigenvalues of $Y_n T_n(f)$ are asymptotically described by a 2×2 matrix-valued function, whose eigenvalue functions are $\pm |f|$. It turns out that roughly half of the eigenvalues of $Y_n T_n(f)$ are well approximated by a uniform sampling of $|f|$ over $[-\pi, \pi]$, while the remaining are well approximated by a uniform sampling of $-|f|$ over the same interval. When f vanishes only on a set of measure zero, this motivates that the spectrum is virtually half positive and half negative. Some insights on the spectral distribution of related preconditioned sequences are provided as well. Finally, a wide number of numerical results illustrate our theoretical findings.

Communicated by Lothar Reichel.

✉ M. Mazza
mariarosa.mazza@ipp.mpg.de

J. Pestana
jennifer.pestana@strath.ac.uk

1 Division of Numerical Methods for Plasma Physics, Max Planck Institute for Plasma Physics, Boltzmannstrasse 2, 85748 Garching bei München, Germany

2 Department of Mathematics and Statistics, University of Strathclyde, 26 Richmond Street, Glasgow G1 1XH, UK

1 Introduction

Given a Toeplitz matrix $T_n(f) \in \mathbb{R}^{n \times n}$ generated by a function $f \in L^1([-\pi, \pi])$, and the exchange matrix $Y_n \in \mathbb{R}^{n \times n}$,

$$Y_n = \begin{bmatrix} & & & 1 \\ & & 1 & \\ & \cdot^{\cdot^{\cdot}} & & \\ 1 & & & \end{bmatrix},$$

numerical experiments suggest that $Y_n T_n(f)$ has eigenvalues that are distributed like $\pm|f|$, i.e., like the eigenvalues of the matrix-valued symbol

$$g = \begin{bmatrix} 0 & f \\ f^* & 0 \end{bmatrix}, \tag{1.1}$$

where f^* is the conjugate of f. In this paper we seek to explain this observation.

One reason for characterizing the spectra of these flipped matrices relates to the solution of linear systems with Toeplitz coefficient matrices. Since $Y_n T_n(f)$ is symmetric, the resulting linear system may be solved by the MINRES method [18,21] or by preconditioned MINRES [16,17], with its descriptive convergence rate bounds based on eigenvalues (see, e.g., [2, Chapters 2 and 4]). However, whilst there has been significant interest in relating the eigenvalues and singular values of Toeplitz sequences to generating functions, analogous results have not been proved for flipped Toeplitz sequences and corresponding preconditioned ones.

This paper aims to fill this gap. To do so, in Sect. 2 we describe the tools we require, specifically we introduce the class of Generalized locally Toeplitz matrix-sequences and related properties [6]. The main results, that describe the spectra of sequences of (preconditioned) flipped Toeplitz matrices can be found in Sect. 3. Examples that illustrate these theoretical results are in Sect. 4.

2 Preliminaries

In this section we formalize the definition of block Toeplitz and Hankel sequences associated to a matrix-valued Lebesgue integrable function. Moreover, we introduce a class of matrix-sequences containing both block Toeplitz and Hankel sequences known as the block Generalized Locally Toeplitz (GLT) class [5,6]. The properties of block GLT sequences will be used to derive the spectral distribution of (preconditioned) flipped Toeplitz sequences (cf. Definition 2.2).

2.1 Block Toeplitz and Hankel matrices, and their spectral distributions

Let us denote by $L^1([-\pi, \pi], s)$ the space of $s \times s$ matrix-valued functions $f :$ $[-\pi, \pi] \to \mathbb{C}^{s \times s}$, $f = [f_{ij}]_{i,j=1}^s$ with $f_{ij} \in L^1([-\pi, \pi])$, $i, j = 1, \ldots, s$. In Defini-

tion 2.1 we introduce the notion of Toeplitz and Hankel matrix-sequences generated by f.

Definition 2.1 Let $f \in L^1([-\pi, \pi], s)$ and let t_j be its Fourier coefficients

$$t_j = \frac{1}{2\pi} \int_{-\pi}^{\pi} f(\theta) e^{-\mathbf{i} j \theta} \, d\theta \in \mathbb{C}^{s \times s},$$

where the integrals are computed component-wise. Then, the n-th $s \times s$-block Toeplitz matrix associated with f is the matrix of order $\widehat{n} = s \cdot n$ given by

$$T_n(f) = [t_{i-j}]_{i,j=1}^n.$$

Similarly, the n-th $s \times s$-block Hankel matrix associated with f is the following $\widehat{n} \times \widehat{n}$ matrix

$$H_n(f) = [t_{i+j-2}]_{i,j=1}^n.$$

The sets $\{T_n(f)\}_n$ and $\{H_n(f)\}_n$ are called the *sequences of $s \times s$-block Toeplitz and Hankel matrices generated by f*, respectively. The function f is referred to as the *generating function* either of $\{T_n(f)\}_n$ or $\{H_n(f)\}_n$.

The generating function f provides a description of the spectrum of $T_n(f)$, for n large enough in the sense of the following definition.

Definition 2.2 Let $f : [a, b] \to \mathbb{C}^{s \times s}$ be a measurable matrix-valued function with eigenvalues $\lambda_i(f)$ and singular values $\sigma_i(f)$, $i = 1, \ldots, s$. Assume that $\{A_n\}_n$ is a sequence of matrices such that $\dim(A_n) = d_n \to \infty$, as $n \to \infty$ and with eigenvalues $\lambda_j(A_n)$ and singular values $\sigma_j(A_n)$, $j = 1, \ldots, d_n$.

- We say that $\{A_n\}_n$ is *distributed as f over $[a, b]$ in the sense of the eigenvalues,* and we write $\{A_n\}_n \sim_\lambda (f, [a, b])$, if

$$\lim_{n \to \infty} \frac{1}{d_n} \sum_{j=1}^{d_n} F(\lambda_j(A_n)) = \frac{1}{b-a} \int_a^b \frac{\sum_{i=1}^s F(\lambda_i(f(t)))}{s} \, dt, \qquad (2.1)$$

  for every continuous function F with compact support. In this case, we say that f is the *symbol* of $\{A_n\}_n$.
- We say that $\{A_n\}_n$ is *distributed as f over $[a, b]$ in the sense of the singular values,* and we write $\{A_n\}_n \sim_\sigma (f, [a, b])$, if

$$\lim_{n \to \infty} \frac{1}{d_n} \sum_{j=1}^{d_n} F(\sigma_j(A_n)) = \frac{1}{b-a} \int_a^b \frac{\sum_{i=1}^s F(\sigma_i(f(t)))}{s} \, dt, \qquad (2.2)$$

  for every continuous function F with compact support.

Remark 2.1 If f is smooth enough, an informal interpretation of the limit relation (2.1) (resp. (2.2)) is that when n is sufficiently large, then d_n/s eigenvalues (resp. singular values) of A_n can be approximated by a sampling of $\lambda_1(f)$ (resp. $\sigma_1(f)$) on a uniform equispaced grid of the domain $[a, b]$, and so on until the last d_n/s eigenvalues (resp. singular values), which can be approximated by an equispaced sampling of $\lambda_s(f)$ (resp. $\sigma_s(f)$) in the domain.

Remark 2.2 Both Definitions 2.1 and 2.2 can be generalized to the case where f : $[-\pi, \pi]^d \to \mathbb{C}^{s \times s}$, $d > 1$. In this case a Toeplitz (resp. Hankel) sequence associated to f is referred to as multilevel block Toeplitz (resp. Hankel) sequence. Theorems 2.2–2.3 and Proposition 2.2 hold true for $d > 1$, as well.

For Toeplitz matrix-sequences, the following theorem (due to Szegő, Tilli, Zamarashkin, Tyrtyshnikov, ...) holds.

Theorem 2.1 (see [8,20,22]) *Let $\{T_n(f)\}_n$ be a Toeplitz sequence generated by $f \in L^1([-\pi, \pi])$. Then, $\{T_n(f)\}_n \sim_\sigma (f, [-\pi, \pi])$. Moreover, if f is real-valued, then $\{T_n(f)\}_n \sim_\lambda (f, [-\pi, \pi])$.*

In the case where f is a Hermitian matrix-valued function, the previous theorem can be extended as follows:

Theorem 2.2 (see [20]) *Let $f \in L^1([-\pi, \pi], s)$ be a Hermitian matrix-valued function. Then, $\{T_n(f)\}_n \sim_\lambda (f, [-\pi, \pi])$.*

We end this subsection with a theorem that is a useful tool for computing the spectral distribution of a sequence of Hermitian matrices. For the related proof, see [11, Theorem 4.3]. From now on, the conjugate transpose of the matrix A is denoted by A^*.

Theorem 2.3 *Let $\{X_n\}_n$ be a sequence of matrices, with X_n Hermitian of size d_n, and let $\{P_n\}_n$ be a sequence such that $P_n \in \mathbb{C}^{d_n \times \delta_n}$, $P_n^* P_n = I_{\delta_n}$, $\delta_n \le d_n$ and $\delta_n/d_n \to 1$ as $n \to \infty$. Then $\{X_n\}_n \sim_\lambda f$ if and only if $\{P_n^* X_n P_n\}_n \sim_\lambda f$.*

2.2 Block generalized locally Toeplitz class

In the sequel, we introduce the block GLT class [5], a *-algebra of matrix-sequences containing both block Toeplitz and Hankel matrix-sequences. The formal definition of block GLT matrix-sequences is rather technical and involves somewhat cumbersome notation: therefore we just give and briefly discuss a few properties of the block GLT class, which are sufficient for studying the spectral features of (preconditioned) flipped Toeplitz matrices.

Throughout, we use the following notation

$$\{A_n\}_n \sim_{\text{GLT}} \kappa(x, \theta), \quad \kappa : [0, 1] \times [-\pi, \pi] \to \mathbb{C}^{s \times s},$$

to say that the sequence $\{A_n\}_n$ is a $s \times s$-block GLT sequence with GLT symbol $\kappa(x, \theta)$.

Here we list four main features of block GLT sequences.

GLT1 Let $\{A_n\}_n \sim_{\text{GLT}} \kappa$ with $\kappa : G \to \mathbb{C}^{s \times s}$, $G = [0, 1] \times [-\pi, \pi]$, then $\{A_n\}_n \sim_\sigma (\kappa, G)$. If the matrices A_n are Hermitian, then it also holds that $\{A_n\}_n \sim_\lambda (\kappa, G)$.

GLT2 The set of block GLT sequences forms a $*$-algebra, i.e., it is closed under linear combinations, products, inversion, conjugation. In formulae, let $\{A_n\}_n \sim_{\text{GLT}} \kappa_1$ and $\{B_n\}_n \sim_{\text{GLT}} \kappa_2$, then

- $\{\alpha A_n + \beta B_n\}_n \sim_{\text{GLT}} \alpha \kappa_1 + \beta \kappa_2, \quad \alpha, \beta \in \mathbb{C}$;
- $\{A_n B_n\}_n \sim_{\text{GLT}} \kappa_1 \kappa_2$;
- $\{A_n^{-1}\}_n \sim_{\text{GLT}} \kappa_1^{-1}$ provided that κ_1 is invertible a.e.;
- $\{A_n^*\}_n \sim_{\text{GLT}} \kappa_1^*$.

GLT 3 Any sequence of block Toeplitz matrices $\{T_n(f)\}_n$ generated by a function $f \in L^1([-\pi, \pi], s)$ is a $s \times s$-block GLT sequence with symbol $\kappa(x, \theta) = f(\theta)$.

GLT4 Let $\{A_n\}_n \sim_\sigma 0$. We say that $\{A_n\}_n$ is a *zero-distributed matrix-sequence*. Note that for any $s > 1$ $\{A_n\}_n \sim_\sigma O_s$, with O_s the $s \times s$ null matrix, is equivalent to $\{A_n\}_n \sim_\sigma 0$. Every zero-distributed matrix-sequence is a block GLT sequence with symbol O_s and viceversa, i.e., $\{A_n\}_n \sim_\sigma 0 \iff \{A_n\}_n \sim_{\text{GLT}} O_s$.

According to Definition 2.2, in the presence of a zero-distributed sequence the singular values of the n-th matrix (weakly) cluster around 0. This is formalized in the following result [6].

Proposition 2.1 *Let $\{A_n\}_n$ be a matrix sequence with A_n of size d_n with $d_n \to \infty$, as $n \to \infty$. Then $\{A_n\}_n \sim_\sigma 0$ if and only if there exist two matrix sequences $\{R_n\}_n$ and $\{E_n\}_n$ such that $A_n = R_n + E_n$, and*

$$\lim_{n \to \infty} \frac{\text{rank}(R_n)}{d_n} = 0, \qquad \lim_{n \to \infty} \|E_n\| = 0,$$

where $\| \cdot \|$ is the spectral norm.

We next recall a result on the spectral distribution of Hankel sequences associated to $f \in L^1([-\pi, \pi], s)$.

Proposition 2.2 (see [3]) *If $\{H_n(f)\}_n$ is an Hankel sequence generated by $f \in L^1([-\pi, \pi], s)$, then $\{H_n(f)\}_n \sim_\sigma 0$.*

Proposition 2.2 together with **GLT4** tell us that $\{H_n(f)\}_n$ is a $s \times s$-block GLT sequence with symbol O_s.

We end this preliminary section with a theorem that is very useful in the context of GLT preconditioning. It is obtained as a straightforward extension of Theorem 1 in [7] to the block GLT case where the symbol of the preconditioning sequence is a multiple of the identity.

Theorem 2.4 *Let $\{A_n\}_n$ be a sequence of Hermitian matrices such that $\{A_n\}_n \sim_{\text{GLT}} \kappa$, with $\kappa : G \to \mathbb{C}^{s \times s}$, $G = [0, 1] \times [-\pi, \pi]$, and let $\{\mathcal{P}_n\}_n$ be a sequence of Hermitian positive definite matrices such that $\{\mathcal{P}_n\}_n \sim_{\text{GLT}} h \cdot I_s$, with $h : G \to \mathbb{C}$, such that $h \neq 0$ a.e. Then*

$$\{\mathcal{P}_n^{-1} A_n\}_n \sim_{\sigma, \lambda} (h^{-1} \kappa, G).$$

3 Spectral distribution of (preconditioned) flipped Toeplitz sequences

To characterize the spectral distribution of $Y_n T_n(f)$ we will subdivide $T_n(f)$ into a 2×2 block matrix as follows:

$$
T_n(f) = \begin{matrix} & n-m & m & \\ & \begin{bmatrix} T_{11} & T_{12} \\ T_{21} & T_{22} \end{bmatrix} & \begin{matrix} m \\ n-m \end{matrix} \end{matrix}, \tag{3.1}
$$

where $m = \lfloor n/2 \rfloor$. Note that when $n = 2m$, $m \in \mathbb{N}$, i.e., n is even, $T_{2m}(f)$ is made of four square blocks. However, when n is odd only the blocks $(1, 2)$ and $(2, 1)$ on the anti-diagonal are square matrices of size $m \times m$ and $n - m \times n - m$, respectively. Applying Y_n to $T_n(f)$ in (3.1) gives

$$
Y_n T_n(f) = \begin{bmatrix} Y_{n-m} T_{21} & Y_{n-m} T_{22} \\ Y_m T_{11} & Y_m T_{12} \end{bmatrix}.
$$

Furthermore, we can apply a similarity transform to $Y_n T_n(f)$ using the matrix

$$
U_n = \begin{bmatrix} Y_{n-m} & \\ & I_m \end{bmatrix}.
$$

This gives

$$
G_n = U_n Y_n T_n(f) U_n = \underbrace{\begin{bmatrix} T_{21} Y_{n-m} & \\ & Y_m T_{12} \end{bmatrix}}_{M_n} + \underbrace{\begin{bmatrix} & T_{22} \\ Y_m T_{11} Y_{n-m} & \end{bmatrix}}_{\widehat{T}_n}. \tag{3.2}
$$

When $n = 2m$, by using the fact that $T_{11} = T_{22} = T_m(f)$ and $Y_m T_{11} Y_m = T_m^T(f)$, we can split G_{2m} as follows:

$$
G_{2m} = \underbrace{\begin{bmatrix} T_{21} Y_m & \\ & Y_m T_{12} \end{bmatrix}}_{M_n} + \underbrace{\begin{bmatrix} & T_m(f) \\ T_m^T(f) & \end{bmatrix}}_{\widehat{T}_n}. \tag{3.3}
$$

In the following lemmas we prove that $\{M_n\}_n \sim_\lambda 0$ and that $\{\widehat{T}_n\}_n \sim_\lambda (g, [-\pi, \pi])$ with g as in (1.1). The proof of Lemma 3.1 is based on the idea in Proposition 3.10 in [10].

Lemma 3.1 *Let* $\{T_n(f)\}_n$, $T_n(f) \in \mathbb{R}^{n \times n}$ *be the Toeplitz sequence associated to* $f \in L^1([-\pi, \pi])$, *and let* M_n *be defined as in* (3.2) *when n is odd and as in* (3.3) *when n is even. Then,* $M_n = R_n + E_n$, *with*

$$
\lim_{n \to \infty} \frac{\mathrm{rank}(R_n)}{n} = 0, \qquad \lim_{n \to \infty} \|E_n\| = 0. \tag{3.4}
$$

Moreover,

$$\{M_n\}_n \sim_{\text{GLT},\sigma,\lambda} 0.$$

Proof Let us begin with the case that $n = 2m$. Then, (3.3) shows that

$$M_{2m} = \begin{bmatrix} T_{21}Y_m & \\ & Y_m T_{12} \end{bmatrix}.$$

Now,

$$T_{21}Y_m = \begin{bmatrix} t_1 & \cdots & t_{m-1} & t_m \\ t_2 & \cdots & t_m & t_{m+1} \\ \vdots & \ddots & \vdots & \vdots \\ t_m & \cdots & t_{n-2} & t_{n-1} \end{bmatrix},$$

which is a submatrix of

$$H_{m+1}(f) = \begin{bmatrix} t_0 & t_1 & \cdots & t_{m-1} & t_m \\ t_1 & t_2 & \cdots & t_m & t_{m+1} \\ \vdots & \vdots & \ddots & \vdots & \vdots \\ t_{m-1} & t_m & \cdots & t_{n-2} & t_{n-1} \\ t_m & t_{m+1} & \cdots & t_{n-1} & t_n \end{bmatrix},$$

i.e.,

$$\begin{bmatrix} \mathbf{0} & T_{21}Y_m \\ 0 & \mathbf{0}^T \end{bmatrix} = H_{m+1}(f) + U_1 V_1^T, \tag{3.5}$$

where $U_1, V_1 \in \mathbb{R}^{(m+1)\times 2}$.

We want to write down a similar decomposition for $Y_m T_{12}$. To so do, we first note that since $T_n(f)$ is real,

$$t_{-k} = (t_{-k})^* = \frac{1}{2\pi} \int_{-\pi}^{\pi} \left(f(\theta)\, e^{ik\theta} \right)^* d\theta = \frac{1}{2\pi} \int_{-\pi}^{\pi} f^*(\theta)\, e^{-ik\theta}\, d\theta,$$

which is the k-th Fourier coefficient of $f^*(\theta)$. Moreover, $f^*(\theta) = f(-\theta)$.

Thus,

$$Y_m T_{12} = \begin{bmatrix} t_{-1} & t_{-2} & \cdots & t_{-m} \\ \vdots & \vdots & \ddots & \vdots \\ t_{1-m} & t_{-m} & \cdots & t_{2-n} \\ t_{-m} & t_{-m-1} & \cdots & t_{1-n} \end{bmatrix},$$

which is a submatrix of

$$H_{m+1}(f^*) = \begin{bmatrix} t_0 & t_{-1} & t_{-2} & \cdots & t_{-m} \\ \vdots & \vdots & \vdots & \ddots & \vdots \\ t_{2-m} & t_{1-m} & t_{-m} & \cdots & t_{2-n} \\ t_{1-m} & t_{-m} & t_{-m-1} & \cdots & t_{1-n} \\ t_{-m} & t_{-m-1} & \cdots & t_{1-n} & t_{-n} \end{bmatrix},$$

so that

$$\begin{bmatrix} \mathbf{0} & Y_m T_{12} \\ 0 & \mathbf{0}^T \end{bmatrix} = H_{m+1}(f^*) + U_2 V_2^T, \tag{3.6}$$

where $U_2, V_2 \in \mathbb{R}^{(m+1)\times 2}$.

Thanks to (3.5) and (3.6), we can write M_n as a submatrix of

$$\widetilde{M}_{n+2} = \begin{bmatrix} H_{m+1}(f) & \\ & H_{m+1}(f^*) \end{bmatrix} + \begin{bmatrix} U_1 V_1^T & \\ & U_2 V_2^T \end{bmatrix}.$$

Note that the first term of $\widetilde{M}_{n+2}$ is a permutation of a 2×2-block Hankel matrix, i.e.,

$$\Pi \begin{bmatrix} H_{m+1}(f) & \\ & H_{m+1}(f^*) \end{bmatrix} \Pi^T = H_{n+2}(\widetilde{g}), \quad \widetilde{g} = \begin{bmatrix} f & 0 \\ 0 & f^* \end{bmatrix}.$$

To write explicitly the permutation matrix Π, let us define by e_j, $j = 1, \ldots, 2(m+1)$ the j-th column of the identity matrix of size $2(m+1)$ and by π_j, $j = 1, \ldots, 2(m+1)$ the j-th column of Π. Then,

$$\pi_j = \begin{cases} e_{2j-1} & j = 1, \ldots, m+1, \\ e_{2(j-(m+1))} & j = m+2, \ldots, 2(m+1). \end{cases} \tag{3.7}$$

As a consequence, $\widetilde{M}_{n+2}$ is the sum of a permutation of $H_{n+2}(\widetilde{g})$ plus a matrix whose rank is fixed to 4. Thus, by Propositions 2.1–2.2, we have $\widetilde{M}_{n+2} = \widetilde{R}_{n+2} + \widetilde{E}_{n+2}$ with

$$\lim_{n \to 0} \frac{\text{rank}(\widetilde{R}_{n+2})}{n+2} = 0, \qquad \lim_{n \to 0} \|\widetilde{E}_{n+2}\| = 0.$$

Therefore, we get $M_{2m} = R_{2m} + E_{2m}$, with R_{2m} and E_{2m} submatrices of $\widetilde{R}_{n+2}$ and $\widetilde{E}_{n+2}$, respectively. Since $\text{rank}(R_{2m}) \leq \text{rank}(\widetilde{R}_{n+2})$ and $\|E_{2m}\| \leq \|\widetilde{E}_{n+2}\|$ we have

$$\lim_{n \to \infty} \frac{\text{rank}(R_{2m})}{n} = 0, \qquad \lim_{n \to \infty} \|E_{2m}\| = 0,$$

and this completes the proof of (3.4) when n is even. To prove that (3.4) holds also when n is odd, i.e., $n = 2m + 1$ it is enough to observe that now

$$M_{2m+1} = \begin{bmatrix} T_{21} Y_{m+1} & \\ & Y_m T_{12} \end{bmatrix},$$

with

$$T_{21} Y_{m+1} = \begin{bmatrix} t_0 & \cdots & t_{m-1} & t_m \\ t_1 & \cdots & t_m & t_{m+1} \\ \vdots & \ddots & \vdots & \vdots \\ t_m & \cdots & t_{n-2} & t_{n-1} \end{bmatrix} = H_{m+1}(f),$$

while

$$Y_m T_{12} = \begin{bmatrix} t_{-2} & \dots & t_{-m-1} \\ \vdots & \ddots & \vdots \\ t_{-m-1} & \dots & t_{1-n} \end{bmatrix},$$

which is a submatrix of

$$H_{m+1}(f^*) = \begin{bmatrix} t_0 & t_{-1} & t_{-2} & \dots & t_{-m} \\ t_{-1} & t_{-2} & t_{-3} & \dots & t_{-m-1} \\ \vdots & \vdots & \vdots & \ddots & \vdots \\ t_{1-m} & t_{-m} & t_{-m-1} & \dots & t_{2-n} \\ t_{-m} & t_{-m-1} & \dots & t_{2-n} & t_{1-n} \end{bmatrix},$$

so that

$$\begin{bmatrix} 0 & \mathbf{0}^T \\ \mathbf{0} & Y_m T_{12} \end{bmatrix} = H_{m+1}(f^*) + U_3 V_3^T,$$

where $U_3, V_3 \in \mathbb{R}^{(m+1)\times 2}$. The above reasoning for the case $n = 2m$ then shows that (3.4) is true when n is odd.

Proposition 2.1 shows that

$$\{M_n\}_n \sim_\sigma 0.$$

Then, **GLT4** implies that $\{M_n\}_n \sim_{GLT} 0$. The proof is complete once we note that M_n is real symmetric: thanks to **GLT1** this implies that $\{M_n\}_n$ is distributed as 0 also in the eigenvalue sense. $\quad\square$

The following lemma concerns the spectral distribution of the matrix-sequence $\{\widehat{T}_n\}_n$.

Lemma 3.2 *Let* $\{T_n(f)\}_n$, $T_n(f) \in \mathbb{R}^{n\times n}$ *be the Toeplitz sequence associated to* $f \in L^1([-\pi, \pi])$, *and let* $\{\widehat{T}_n\}_n$ *be defined as in* (3.2) *when n is odd and as in* (3.3) *when n is even. Then,*

$$\{\widehat{T}_n\}_n \sim_\lambda (g, [-\pi, \pi]), \text{ with } g = \begin{bmatrix} 0 & f \\ f^* & 0 \end{bmatrix}.$$

Proof Let us assume first that $n = 2m$. Then,

$$\widehat{T}_{2m} = \begin{bmatrix} & T_m(f) \\ T_m^T(f) & \end{bmatrix}.$$

By using the same permutation matrix Π as in (3.7) with m in place of $m + 1$, we can rewrite $\widehat{T}_{2m}$ as a 2×2-block Toeplitz matrix, i.e.,

$$\Pi \widehat{T}_{2m} \Pi^T = T_{2m}(g), \text{ with } g = \begin{bmatrix} 0 & f \\ f^* & 0 \end{bmatrix}.$$

Due to the fact that g is an Hermitian matrix-valued function and thanks to Theorem 2.2 with $s = 2$, we have

$$\{\widehat{T}_{2m}\}_n \sim_\lambda (g, [-\pi, \pi]), \text{ with } g = \begin{bmatrix} 0 & f \\ f^* & 0 \end{bmatrix},$$

which completes the proof when n is even. To prove the thesis when n odd we note that

$$\widehat{T}_{2m+1} = \begin{bmatrix} 0 & u^T \\ u & \widehat{T}_{2m} \end{bmatrix},$$

with $u \in \mathbb{R}^{2m}$, i.e., $\widehat{T}_{2m}$ is a principal submatrix of $\widehat{T}_{2m+1}$ of order $2m \times 2m$. By exploiting the fact that $\widehat{T}_{2m+1}$ is real symmetric and by using Theorem 2.3 with $P_n \in \mathbb{R}^{n \times (n-1)}$,

$$P_n = \begin{bmatrix} \mathbf{0}^T \\ I_{n-1} \end{bmatrix},$$

we get

$$\{\widehat{T}_{2m} = P_n^T \widehat{T}_{2m+1} P_n\}_n \sim_\lambda (g, [-\pi, \pi]) \iff \{\widehat{T}_{2m+1}\}_n \sim_\lambda (g, [-\pi, \pi]),$$

and the proof is complete.

We are now ready to present our main results.

Theorem 3.1 *Let* $\{T_n(f)\}_n$, $T_n(f) \in \mathbb{R}^{n \times n}$ *be the Toeplitz sequence associated to* $f \in L^1([-\pi, \pi])$*, and let* $\{Y_n T_n(f)\}_n$ *be the corresponding sequence of flipped Toeplitz matrices. Then,*

$$\{Y_n T_n(f)\}_n \sim_\lambda (g, [-\pi, \pi]), \text{ with } g = \begin{bmatrix} 0 & f \\ f^* & 0 \end{bmatrix}. \tag{3.8}$$

Proof To prove the thesis it is enough to put together Lemmas 3.1–3.2 and to apply **GLT2**.

Remark 3.1 Notice that multiplication by Y_n does not affect the spectral distribution in the singular value sense of the original Toeplitz sequence $\{T_n(f)\}_n$, that is

$$\{Y_n T_n(f)\}_n \sim_\sigma (f, [-\pi, \pi]). \tag{3.9}$$

This immediately follows from the fact that since Y_n is unitary $T_n(f)$ and $Y_n T_n(f)$ have the same singular values.

Remark 3.2 The same argument used for real Toeplitz matrices shows that relation (3.9) still holds for complex Toeplitz matrices. Concerning the eigenvalue distribution, in general we do not expect a symbol as in (3.8). For instance, if we consider the matrix

$T_n(\tilde{f})$, with $\tilde{f} = \mathrm{i}f$ and f such that its Fourier coefficients are real, then by applying Theorem 3.1 to $T_n(f)$, it can be easily seen that

$$\{Y_n T_n(\tilde{f})\}_n \sim_\lambda (\tilde{g}, [-\pi, \pi]), \ \text{with } \tilde{g} = \begin{bmatrix} 0 & \tilde{f} \\ -\tilde{f}^* & 0 \end{bmatrix}.$$

More detailed work for general complex Toeplitz matrices will be the subject of future research.

Remark 3.3 Theorem 3.1 can be easily generalized to certain block Toeplitz matrices by applying the same strategy used in this section. Specifically, given $T_n(f) \in \mathbb{R}^{\hat{n} \times \hat{n}}$, $\hat{n} = s \cdot n$, generated by a matrix-valued function $f \in L^1([-\pi, \pi], s)$, $s > 1$, assume that its Fourier coefficients $\{t_j\}_{j \in \mathbb{Z}}$ are symmetrized by a real symmetric involutory matrix $W_s \in \mathbb{R}^{n \times n}$, so that $W_s t_j = t_j^T W_s$, $j \in \mathbb{Z}$. Then

$$\{\widehat{Y}_n T_n(f)\}_n \sim_\lambda (g, [-\pi, \pi]),$$

where $\widehat{Y}_n \in \mathbb{R}^{\hat{n} \times \hat{n}}$, $\widehat{Y}_n = Y_n \otimes W_s$.

Based on Theorem 3.1 and on Remark 2.1, we expect that asymptotically almost half of the eigenvalues of $Y_n T_n(f)$ are well approximated by a uniform sampling of $|f|$ over $[-\pi, \pi]$, while the remaining are well approximated by a uniform sampling of $-|f|$ over the same interval. Specifically, a certain number of outliers whose ratio is infinitesimal in the matrix-size is allowed. When f vanishes only on a set of measure zero, this motivates that the spectrum is virtually half positive and half negative.

Remark 3.4 Independently, a result equivalent to Theorem 3.1 has been proved in [4]; see Theorem 3.2 and Corollary 3.3 therein. The main differences between the approach used here and the one in [4] can be summarized as follows: in [4] the authors use the notion of approximating class of sequences, a technical tool behind the GLT construction, and they write the symbol as a scalar function (devoting some extra attention to how to define its domain). Here we leverage the block GLT algebra as a black-box tool and we naturally get a matrix-valued symbol with two eigenvalue functions that, in line with Remark 2.1, immediately fits with the quasi-half positive/negative nature of the spectrum of $Y_n T_n(f)$.

We end this section by providing the spectral distribution of a preconditioned sequence of flipped Toeplitz matrices.

Theorem 3.2 *Let $\{T_n(f)\}_n$, $T_n(f) \in \mathbb{R}^{n \times n}$ be the Toeplitz sequence associated to $f \in L^1([-\pi, \pi])$, let $\{Y_n T_n(f)\}_n$ be the corresponding sequence of flipped Toeplitz matrices, and let $\{\mathscr{P}_n\}_n$ be a sequence of Hermitian positive definite matrices such that $\{\mathscr{P}_n\}_n \sim_{\mathrm{GLT}} h$, with $h : [-\pi, \pi] \to \mathbb{C}$ and $h \neq 0$ a.e. Then,*

$$\{\mathscr{P}_n^{-1} Y_n T_n(f)\}_n \sim_\lambda (h^{-1}g, [-\pi, \pi]). \tag{3.10}$$

Proof The thesis easily follows from the combination of Theorem 2.4 with Theorem 3.1 by noticing that $\{\mathscr{P}_n\}_n \sim_{\mathrm{GLT}} h$ is equivalent to $\{\mathscr{P}_n\}_n \sim_{\mathrm{GLT}} h \cdot I_2$, and recalling that $Y_n T_n(f)$ is real symmetric.
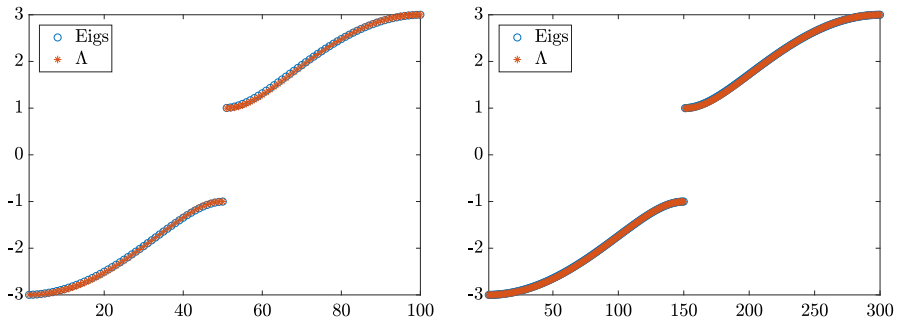
Fig. 1 Comparison of the eigenvalues of $Y_n T_n(f)$ (blue circle) with Λ collecting uniform samples of $\lambda_i(g) = \pm|f(\theta)|$, $i = 1, 2$ (red asterisk), ordered in an ascending way, for Example 4.1 when $n = 100$ (left) and $n = 300$ (right) (colour figure online)

In the next section we give a variety of examples that validate the theoretical findings in Theorems 3.1 and 3.2.

4 Numerical experiments

In this section we provide numerical evidence for the theory developed in Sect. 3. The problems we consider represent banded and dense Toeplitz matrices, some of which come from applications. We start by defining the following equispaced grid on $[0, \pi]$:

$$\Gamma = \left\{ \theta_j = \frac{\pi j}{m - 1}, \quad j = 0, \ldots, m - 1, \quad m = \left\lfloor \frac{n}{2} \right\rfloor \right\}.$$

Then, we denote by Λ_1 and Λ_2 the set of all evaluations of $\lambda_1(g)$, $\lambda_2(g)$ (resp. $\lambda_1(h^{-1}g)$, $\lambda_2(h^{-1}g)$) on Γ, and by Λ the union $\Lambda_1 \cup \Lambda_2$ ordered in an ascending way. In the following examples we numerically check relation (3.8) (resp. (3.10)) by comparing the eigenvalues of $Y_n T_n(f)$ (resp. $\mathscr{P}_n^{-1} Y_n T_n(f)$) with the values collected in Λ. In Examples 4.1–4.4 we also compare the eigenvalues of $Y_n T_n(f)$ directly with the spectrum of g. Note that it suffices to consider only $[0, \pi]$ in place of $[-\pi, \pi]$ because the eigenvalue functions of the considered symbols are even. This is clear for the unpreconditioned case since $T_n(f)$ is real and so $\lambda_i(g) = \pm|f(\theta)| = \pm|f^*(\theta)| = \pm|f(-\theta)|$. The preconditioned case will be discussed in Example 4.7.

Example 4.1 Our first example is the banded Toeplitz matrix generated by $f(\theta) = 2 + e^{i\theta}$. We see from Fig. 1 that, even for small matrices, the sampling of the eigenvalue functions of g collected in Λ accurately describes the eigenvalues of $Y_n T_n(f)$. Also Fig. 2a confirms a good matching between the eigenvalues of $Y_n T_n(f)$ and the spectrum of g when $n = 100$.

Example 4.2 Next, we consider a dense Toeplitz matrix that arises from the discretization of space-fractional diffusion problems. Specifically, they occur when solving
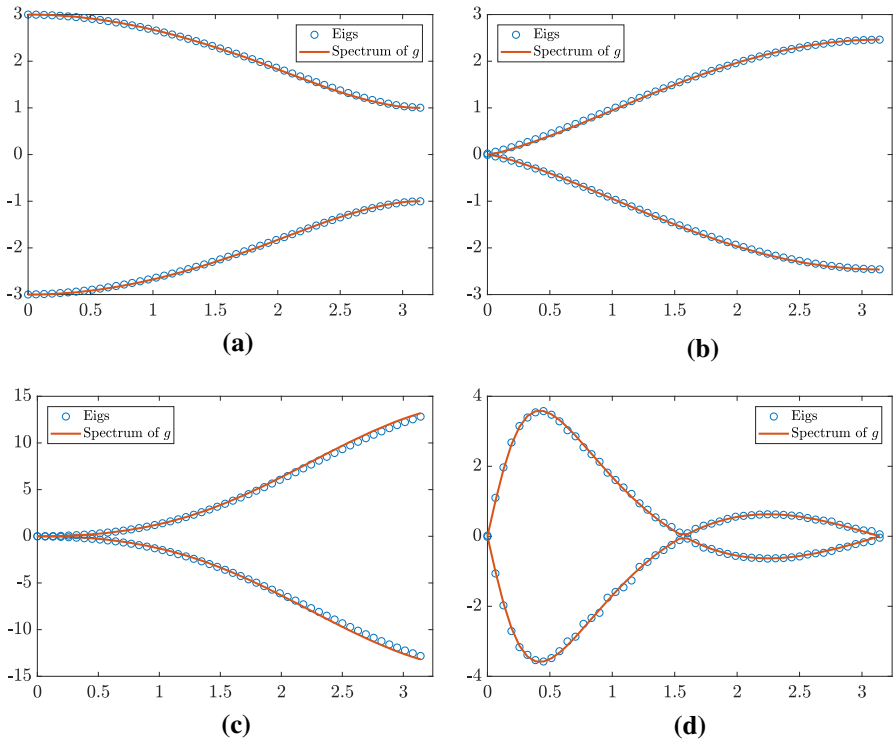
Fig. 2 Eigenvalues of $Y_n T_n(f)$ and the spectrum of g in (3.8) for Example 4.1–Example 4.4 when $n = 100$. **a** Example 4.1, **b** Example 4.2, **c** Example 4.3, **d** Example 4.4

steady-state, or time-dependent, fractional diffusion equations involving the Riemann–Liouville fractional derivatives defined as follows (see, e.g., [1])

$$
\begin{aligned}
\frac{d^\alpha u(x)}{d_+ x^\alpha} &= \frac{1}{\Gamma(n-\alpha)} \frac{d^n}{dx^n} \int_L^x \frac{u(\xi)}{(x-\xi)^{\alpha+1-n}} d\xi, \\
\frac{d^\alpha u(x)}{d_- x^\alpha} &= \frac{(-1)^n}{\Gamma(n-\alpha)} \frac{d^n}{dx^n} \int_x^R \frac{u(\xi)}{(\xi-x)^{\alpha+1-n}} d\xi,
\end{aligned}
\tag{4.1}
$$

where n is the integer for which $n - 1 < \alpha \le n$, and $x \in [L, R]$.

After discretizing these derivatives by a shifted Grünwald-Letnikov finite difference method [12,13], we obtain an approximation of $\frac{d^\alpha u(x)}{d_+ x^\alpha}$. For instance, when the step size is constant, the approximation of $\frac{d^\alpha u(x)}{d_+ x^\alpha}$ is a dense lower Hessenberg Toeplitz matrix $T_n(f)$, with symbol $f(\theta) = e^{-i\theta}(1 + e^{i(\pi+\theta)})^\alpha$ as described in [1]. Figure 3 shows that when $n = 100$ the eigenvalues of the flipped Toeplitz matrix $Y_n T_n(f)$ are well described by the sampling of the eigenvalue functions of g collected in Λ, and when $n = 300$ the two are visually indistinguishable. Similar results can be inferred from Fig. 2b when comparing the eigenvalues of $Y_n T_n(f)$ directly with the spectrum of g.
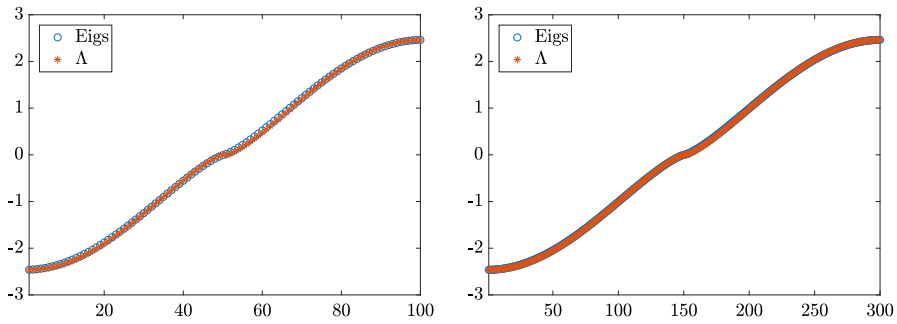
Fig. 3 Comparison of the eigenvalues of $Y_n T_n(f)$ (blue circle) with Λ collecting uniform samples of $\lambda_i(g) = \pm|f(\theta)|$, $i = 1, 2$ (red asterisk), ordered in an ascending way, for Example 4.2 when $n = 100$ (left) and $n = 300$ (right) (colour figure online)
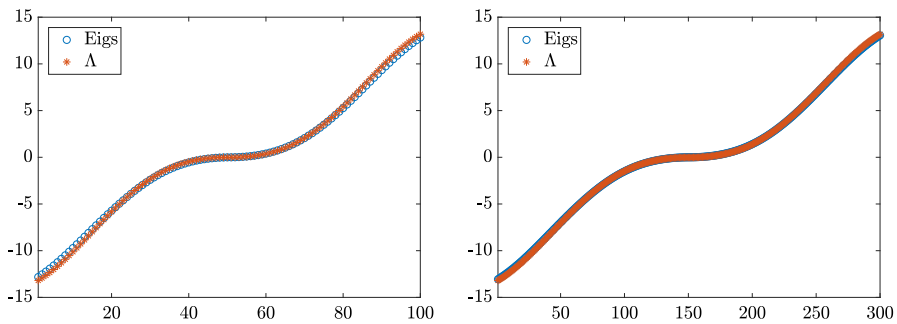

Fig. 4 Comparison of the eigenvalues of $Y_n T_n(f)$ (blue circle) with Λ collecting uniform samples of $\lambda_i(g) = \pm|f(\theta)|$, $i = 1, 2$ (red asterisk), ordered in an ascending way, for Example 4.3 when $n = 100$ (left) and $n = 300$ (right) (colour figure online)

Example 4.3 This example from [9, Example 2] has dense Toeplitz matrices with slowly decaying entries. These entries are defined by the generating function $f(\theta) = (2 - 2\cos(\theta))(1 + \mathbf{i}x)$. Figure 4 illustrates that even for such matrices the sampling of the eigenvalue functions of g collected in Λ accurately describes the eigenvalues of $Y_n T_n(f)$. We refer the reader to Fig. 2c for the direct comparison with the spectrum of g.

Example 4.4 In our fourth example, we choose the rational generating function

$$f(\theta) = \frac{e^{4\mathbf{i}\theta} - 1}{\left(e^{\mathbf{i}\theta} - \frac{3}{2}\right)\left(e^{\mathbf{i}\theta} - \frac{1}{2}\right)}$$

from [14, Example 10].

The eigenvalues of $Y_n T_n(f)$ are again characterized by a uniform sampling of the eigenvalues of g (see Fig. 5), even though the spectrum is somewhat more complicated than in previous examples (see Fig. 2d).
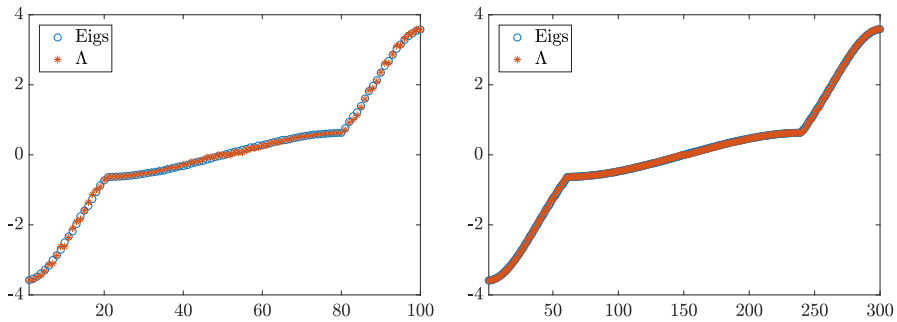
Fig. 5 Comparison of the eigenvalues of $Y_n T_n(f)$ (blue circle) with Λ collecting uniform samples of $\lambda_i(g) = \pm |f(\theta)|$, $i = 1, 2$ (red asterisk), ordered in an ascending way, for Example 4.4 when $n = 100$ (left) and $n = 300$ (right) (colour figure online)

Example 4.5 In this example we consider the Toeplitz sequences generated by the symbol of the advection and mass matrices encountered, for instance, when dealing with a Galerkin B-spline isogeometric discretization of convection-diffusion-reaction equations (refer to [6, pp. 235–239] for a detailed discussion). More precisely, if we denote the mesh size by n and the B-spline degree by the fixed value p, we take $\{T_{n+p}(a_p)\}_n$ and $\{T_{n+p}(m_p)\}_n$ with

$$a_p(\theta) = -2 \sum_{k=1}^{p} \phi'_{2p+1}(p + 1 - k) \sin(k\theta),$$

$$m_p(\theta) = \phi_{2p+1}(p + 1) + 2 \sum_{k=1}^{p} \phi_{2p+1}(p + 1 - k) \cos(k\theta),$$

where ϕ_{2p+1} is the cardinal B-spline on knots $\{0, 1, \ldots, 2p+2\}$. Note that the advection Toeplitz sequence $\{T_{n+p}(a_p)\}_n$ is made of complex (skew-symmetric) matrices whose symbol satisfies the conditions in Remark 3.2, while the matrices of the mass Toeplitz sequence $\{T_{n+p}(m_p)\}_n$ are symmetric.

Let $\tilde{g}$ be the symbol of $\{Y_{n+p} T_{n+p}(a_p)\}_n$. In Fig. 6a, we set p to 4 and we compare the imaginary part of the eigenvalues of $Y_{n+p} T_{n+p}(a_p)$ with a sampling of $\pm |a_p|$, i.e., with the imaginary part of $\lambda_i(\tilde{g})$, $i = 1, 2$ over $[0, \pi]$. We refer to the resulting set ordered in an ascending way as $\tilde{\Lambda}$. As in all previous examples, the matching between the two is quite good when $n = 300$. Similar results can be obtained when comparing the eigenvalues of $Y_{n+p} T_{n+p}(m_p)$ with a sampling of $\pm |m_p|$ over $[0, \pi]$ (refer to Fig. 6b).

Example 4.6 In all previous examples, the matching between eigenvalues and the sampling of the eigenvalue functions was "exact", in the sense that there were no outliers. In our final example we show a case where the outliers come into play. More precisely, we show how to build sequences of matrices with a constant number of outliers that can be chosen a priori.
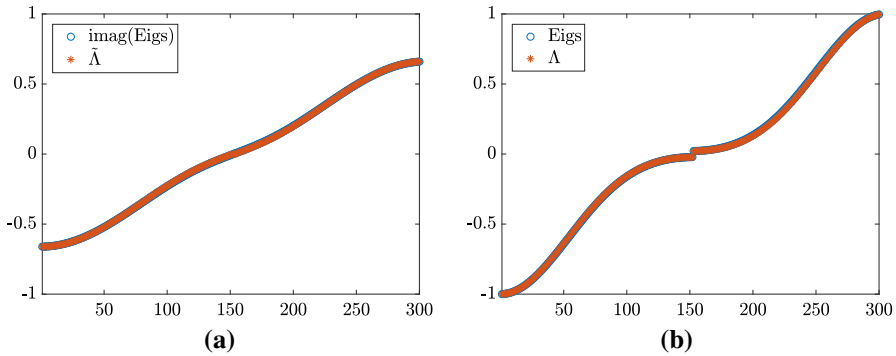
Fig. 6 a Comparison of the imaginary part of the eigenvalues of $Y_{n+p}T_{n+p}(f)$ (blue circle) with $\tilde{\Lambda}$ collecting uniform samples of $\pm|a_p|$ (red asterisk), ordered in an ascending way for Example 4.5 when $f = a_p$, $p = 4$, and $n = 300$; **b** comparison of the eigenvalues of $Y_{n+p}T_{n+p}(f)$ (blue circle) with Λ collecting uniform samples of $\lambda_i(g) = \pm|m_p|$, $i = 1, 2$ (red asterisk), ordered in an ascending way, for Example 4.5 when $f = m_p$, $p = 4$, and $n = 300$ (colour figure online)

Table 1 Outliers for $T_{n+p}(m_p + r_{p,t})$ when: (a) $p = 3, t = 2$, $n = 100, 200, 400, 800, 1600$; (b) $n = 300, t = 2$, $p = 1, \ldots, 5$; (c) $n = 300$, $p = 4, t = 5, 10, 15, 20, 25$

n	Out.	p	Out.	t	Out.
100	3	1	3	5	9
200	3	2	4	10	14
400	3	3	5	15	19
800	3	4	6	20	24
1600	3	5	7	25	29
	(a)		(b)		(c)

Let us define $r_{p,t}(\theta) = e^{(p+t)i\theta}$, with $t > 1$ and $p \geq 1$, and let us consider the Toeplitz sequence $\{T_{n+p}(m_p + r_{p,t})\}_n$, with m_p as in the previous example. As shown in Table 1a, with the fixed values of $p = 3, t = 2$ and varying n, we get a constant number of outliers equal to 5. More generally, the number of outliers of $T_{n+p}(m_p + r_{p,t})$ equals $p + t$ and can be decided a priori by changing either p or t as illustrated in Table 1b, c.

Example 4.7 Our final example shows how the spectral results in Sect. 3 can be used to describe the convergence rate of preconditioned MINRES, which depends heavily on the spectral properties of the coefficient matrix (see, e.g., [2, Chapters 2 and 4]).

We consider the dense Toeplitz matrix already discussed in Example 4.2 that results from the discretization of the space-fractional diffusion problem in [15, Example 3]:

$$-\frac{d}{dx}\left(\frac{d^{1-\beta} u(x)}{d_+x^{1-\beta}}\right) = 1, \quad 0 < x < 1,$$

with absorbing boundary conditions and $0 < \beta < 1$, where the fractional derivative is defined as in (4.1).

Discretizing Example 4.7 by a shifted Grünwald-Letnikov finite difference method [12,13] with constant step size $\Delta x = \frac{1}{n+1}$ gives the linear system

$$T_n(f)u_n = b_n,$$

where $T_n(f)$ is the dense lower Hessenberg Toeplitz matrix with symbol $f(\theta) = -e^{-i\theta}(1 + e^{i(\pi+\theta)})^\alpha$ (see [1]) and $b_n = (\Delta x)^{2-\beta}[1, 1, \ldots, 1]^T$. Throughout we choose $\beta = 0.3$.

We either solve Example 4.7 without preconditioning, or apply a symmetric positive definite preconditioner $\mathscr{P}_n$, where $\{\mathscr{P}_n\}_n \sim_{\text{GLT}} h$. It is outside the scope of this manuscript to determine the best preconditioner for this problem, and so we simply examine three choices:

- $\mathscr{P}_n = T_n(f_R)$, where $f_R = (f + f^*)/2$, so that $h = f_R$;
- $\mathscr{P}_n = T_n(|f|)$, so that $h = |f|$, and
- the absolute value Strang circulant preconditioner $\mathscr{P}_n = |C_n|$ described in [17]. To compute $|C_n|$ we first form C_n, the Strang circulant preconditioner for $T_n(f)$ [19]. Then $|C_n| = (C_n^T C_n)^{1/2}$ can be cheaply evaluated using fast Fourier transforms. Since C_n is normal its singular values must equal the eigenvalues of $|C_n|$. The fact that $\{C_n\}_n \sim_\sigma |f|$ implies $h = |f|$.

The same argument as for the unpreconditioned case immediately shows that, for the previous three choices, h is even and so the eigenvalue functions of $h^{-1}g$ can be sampled on $[0, \pi]$.

Figure 7 shows that the eigenvalues of $Y_n T_n(f)$ (resp. $\mathscr{P}_n^{-1} Y_n T_n(f)$) are well described by the sampling of the eigenvalue functions of g (resp. $h^{-1}g$) collected in Λ, as predicted by Theorem 3.1 (resp. Theorem 3.2). Moreover, most of the eigenvalues of the preconditioned matrices lie close to 1 and -1. This is particularly evident for $T_n(|f|)^{-1} Y_n T_n(f)$. We note that $|C_n|^{-1} Y_n T_n(f)$ has a single outlying eigenvalue at 74.7 that is not plotted.

Given the eigenvalues in Fig. 7a and the fact that f has a zero at 0, it is not surprising that MINRES applied to Example 4.7 does not converge. On the other hand, from Fig. 7b–d and since $\lambda_i(h^{-1}g)$ is either bounded or equal to ± 1, we expect that preconditioned MINRES with preconditioners $T_n(f_R)$, $T_n(|f|)$ or $|C_n|$ will converge rapidly. To test this, we apply (preconditioned) MINRES to Example 4.7, stopping when the residual norm is reduced by eight orders of magnitude, i.e, when $\|r_k\|_2/\|r_0\|_2 < 10^{-8}$. We see from Table 2 that these iteration counts are exactly what we might expect from the above spectral results: all three preconditioners are optimal, with $T_n(|f|)$ resulting in the lowest iteration counts.

5 Conclusions

We have investigated the spectra of flipped Toeplitz sequences, i.e., the asymptotic spectral behaviour of $\{Y_n T_n(f)\}_n$, where $T_n(f) \in \mathbb{R}^{n \times n}$ is a real Toeplitz matrix
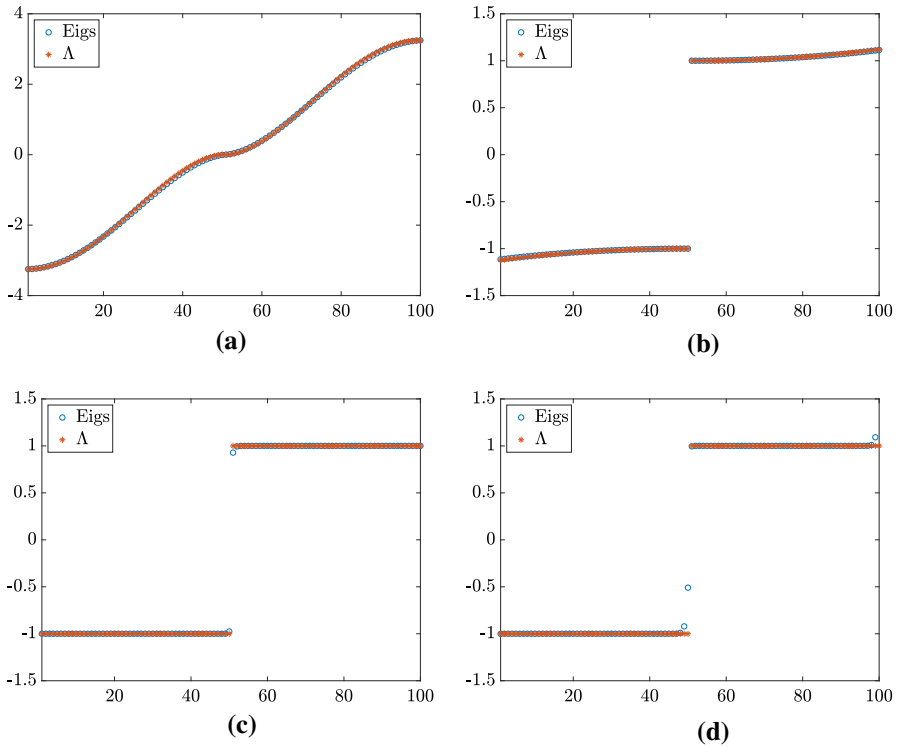
Fig. 7 Comparison of the eigenvalues of $Y_n T_n(f)$ or $\mathscr{P}_n^{-1} Y_n T_n(f))$ (blue circle) with Λ collecting the uniform samples of the eigenvalue functions of g or $h^{-1}g$ for Example 4.7 (red asterisk) when $n = 100$. Note that $|C_n|^{-1} Y_n T_n(f)$ has a single outlying eigenvalue at 74.7 that is not plotted. **a** Unpreconditioned, **b** $\mathscr{P}_n = T_n(f_R)$, **c** $\mathscr{P}_n = T_n(|f|)$, **d** $\mathscr{P}_n = |C_n|$ (colour figure online)

Table 2 Preconditioned MINRES iterations for Example 4.7

n	$T_n(f_R)$	$T_n(|f|)$	$|C_n|$
100	15	7	12
300	16	8	14
500	17	8	15
1000	17	9	15
2000	18	9	17
4000	18	9	17

generated by a function $f \in L^1([-\pi, \pi])$, and Y_n is the exchange matrix, with 1s on the main anti-diagonal. Using the GLT machinery, we have shown that the eigenvalues of $Y_n T_n(f)$ are asymptotically described by a 2×2 matrix-valued function, whose eigenvalue functions are $\pm|f|$. When f vanishes only on a set of measure zero, this motivates that roughly half of the eigenvalues of $Y_n T_n(f)$ are positive, while the remaining are negative. The GLT theory allows us to describe also the asymptotic

spectral behaviour of $\{\mathscr{P}_n^{-1} Y_n T_n(f)\}_n$, when $\mathscr{P}_n$ is Hermitian positive definite, and hence predict the convergence rate of preconditioned MINRES.

References

1. Donatelli, M., Mazza, M., Serra-Capizzano, S.: Spectral analysis and structure preserving preconditioners for fractional diffusion equations. J. Comput. Phys. **307**, 262–279 (2016)
2. Elman, H., Silvester, D., Wathen, A.: Finite Elements and Fast Iterative Solvers with Applications in Incompressible Fluid Dynamics, 2nd edn. Oxford University Press, Oxford (2014)
3. Fasino, D., Tilli, P.: Spectral clustering properties of block multilevel Hankel matrices. Linear Algebra Appl. **306**, 155–163 (2000)
4. Ferrari, P., Furci, I., Hon, S., Mursaleen, M.A., Serra-Capizzano, S.: The eigenvalue distribution of special 2-by-2 block matrix sequences, with applications to the case of symmetrized Toeplitz structures, arXiv:1810.03326 (2018)
5. Garoni, C., Mazza, M., Serra-Capizzano, S.: Block generalized locally Toeplitz sequences: from the theory to the applications. Axioms **7**(3), 49 (2018)
6. Garoni, C., Serra-Capizzano, S.: Generalized Locally Toeplitz Sequences: Theory and Applications, vol. I. Springer, Cham (2017)
7. Garoni, C., Serra-Capizzano, S.: Generalized locally Toeplitz sequences: a spectral analysis tool for discretized differential equations. In: Lyche, T., Manni, C., Speleers, H. (eds.) Splines and PDEs: From Approximation Theory to Numerical Linear Algebra, pp. 161–236. Springer (2018)
8. Grenander, U., Szegő, G.: Toeplitz Forms and Their Applications, vol. 321, 2nd edn. Chelsea, New York (1984)
9. Huckle, T., Serra Capizzano, S., Tablino-Possio, C.: Preconditioning strategies for non-Hermitian Toeplitz linear systems. Numer. Linear Algebra Appl. **12**, 211–220 (2005)
10. Massei, S., Mazza, M., Robol, L.: Fast solvers for 2D fractional diffusion equations using rank structured matrices, arXiv:1804.05522 (2018)
11. Mazza, M., Ratnani, A., Serra-Capizzano, S.: Spectral analysis and spectral symbol for the 2d curl-curl (stabilized) operator with applications to the related iterative solutions. Comput. Math. (2018). https://doi.org/10.1090/mcom/3366
12. Meerschaert, M.M., Tadjeran, C.: Finite difference approximations for fractional advection-dispersion flow equations. J. Comput. Appl. Math. **172**, 65–77 (2004)
13. Meerschaert, M.M., Tadjeran, C.: Finite difference approximations for two-sided space-fractional partial differential equations. Appl. Numer. Math. **56**, 80–90 (2006)
14. Oseledets, I., Tyrtyshnikov, E.: A unifying approach to the construction of circulant preconditioners. Linear Algebra Appl. **418**, 435–449 (2006)
15. Pan, J., Ng, M., Wang, H.: Fast preconditioned iterative methods for finite volume discretization of steady-state space-fractional diffusion equations. Numer. Alg. **74**, 153–173 (2017)
16. Pestana, J.: Preconditioners for symmetrized Toeplitz and multilevel Toeplitz matrices, arXiv:1812.02479 (2018)
17. Pestana, J., Wathen, A.J.: A preconditioned MINRES method for nonsymmetric Toeplitz matrices. SIAM J. Matrix Anal. Appl. **36**, 273–288 (2015)
18. Sogabe, T., Zheng, B., Hashimoto, K., Zhang, S.-L.: A preconditioner of permutation matrix for solving nonsymmetric Toeplitz linear systems. Trans. Jpn. Soc. Ind. Appl. Math. **15**, 159–168 (2004)
19. Strang, G.: A proposal for Toeplitz matrix calculations. Stud. Appl. Math. **74**, 171–176 (1986)
20. Tilli, P.: A note on the spectral distribution of Toeplitz matrices. Linear Multilin. Algebra **45**(2–3), 147–159 (1998)

21. Wang, S.-F., Huang, T.-Z., Gu, X.-M., Luo, W.-H.: Fast permutation preconditioning for fractional diffusion equations. SpringerPlus **5**, 1109 (2016)
22. Zamarashkin, N.L., Tyrtyshnikov, E.E.: Distribution of eigenvalues and singular values of Toeplitz matrices under weakened conditions on the generating function. Sbornik Math. **188**(8), 1191 (1997)